Title

Variation in isotopologues of atmospheric nitric acid in passively collected samples along an air pollution gradient in southern California

Authors

Bell, Michael D
Sickman, James O
Bytnerowicz, Andrzej
et al.

Publication Date

2014-09-01

DOI

10.1016/j.atmosenv.2014.05.031

Peer reviewed

Atmospheric Environment 94 (2014) 287–296

Contents lists available at ScienceDirect

Atmospheric Environment

journal homepage: www.elsevier.com/locate/atmosenv

Variation in isotopologues of atmospheric nitric acid in passively collected samples along an air pollution gradient in southern California

Michael D. Bell [a,*], James O. Sickman [b], Andrzej Bytnerowicz [c], Pamela E. Padgett [c], Edith B. Allen [a]

[a] University of California, Riverside, Department of Botany and Plant Sciences, 900 University Avenue, Riverside, CA 92521, United States
[b] University of California, Riverside, Department of Environmental Science, 900 University Avenue, Riverside, CA 92521, United States
[c] USDA Forest Service, Pacific Southwest Research Station, 4955 Canyon Crest Drive, Riverside, CA 92507, United States

HIGHLIGHTS

- In a stable environment Nylasorb nylon filters collect unbiased HNO_3 $\delta^{15}N$ and $\delta^{18}O$.
- Isotopologues of HNO_3 are depleted at the low end the atm. nitrogen gradient.
- Lightning creates pulses of HNO_3 with a distinctive isotopic signature.
- Patterns in HNO_3 isotopes result from the mixing of HNO_3 sources.

ARTICLE INFO

Article history:
Received 1 November 2013
Received in revised form
6 May 2014
Accepted 9 May 2014
Available online 13 May 2014

Keywords:
Nylasorb nylon filter
Atmospheric deposition
Passive sampler
Nitric acid
$\delta^{15}N$
$\delta^{18}O$
Lightning

ABSTRACT

The sources and oxidation pathways of atmospheric nitric acid (HNO_3) can be evaluated using the isotopic signatures of oxygen (O) and nitrogen (N). This study evaluated the ability of Nylasorb nylon filters to passively collect unbiased isotopologues of atmospheric HNO_3 under controlled and field conditions. Filters contained in passive samplers were exposed in continuous stirred tank reactors (CSTRs) at high (16 $\mu g/m^3$) and moderate (8 $\mu g/m^3$) HNO_3 concentrations during 1–4 week deployment times. Filters were concurrently exposed at high and low N deposition sites along a gradient in the Sonoran Desert. Filters deployed in CSTRs at moderate HNO_3 concentrations for 1–2 weeks had greater variation of $\delta^{18}O$ relative to the 3–4 week deployments, while high concentration samples were consistent across weeks. All deployment means were within 2‰ of the source solution. The $\delta^{15}N$ of all weekly samples were within 0.5‰ of the source solution. Thus, when deployed for longer than 3 weeks, Nylasorb filters collected an isotopically unbiased sample of atmospheric HNO_3. The initial HNO_3 samples at the high deposition field sites had higher $\delta^{15}N$ and $\delta^{18}O$ values than the low deposition sites, suggesting either two independent sources of HNO_3 were mixing or that heavier isotopologues of HNO_3 were preferentially lost from the gas phase through physical deposition or equilibrium chemical reactions. Subsequent HNO_3 samples were subject to summer monsoon conditions leading to variation of isotopic signatures of N and O following 2-source mixing dynamics. Both sites mixed with a source that dominated during the two discrete precipitation events. The high number of lightning strikes near the samplers during the monsoon events suggested that lightning-created HNO_3 was one of the dominant mixing sources with an approximate isotopic signature of 21.6‰ and −0.6‰ for $\delta^{18}O$ and $\delta^{15}N$ respectively. Two-source mixing models suggest that lightning-created HNO_3 made up between 40 and 42% of atmospheric HNO_3 at the high deposition sites and 59–63% at the low deposition during the 4 week exposure.

1. Introduction

Nitrogen emissions from anthropogenic sources (e.g. fertilizers, domestic animal wastes, and internal combustion engines) contribute to the formation of photochemical smog and

* Corresponding author. University of California, Irvine, Center for Environmental Biology, 243 Steinhaus Hall, Irvine, CA 92697, United States.
E-mail address: bellmd@uci.edu (M.D. Bell).

http://dx.doi.org/10.1016/j.atmosenv.2014.05.031
1352-2310/

atmospheric particulates leading to the long distance transport of reactive nitrogen (N) (Fenn et al., 2003; Galloway et al., 2003; Vitousek et al., 1997). Advances in stable isotopic analysis of N and O within atmospheric pollution are increasing our ability to differentiate these sources of N and the formation pathway of nitric acid (HNO_3) (Elliott et al., 2009; Hastings et al., 2003; Templer and Weathers, 2011). The dominant forms of anthropogenic N in Southern California are ammonia (NH_3), nitric oxide (NO), nitrogen dioxide (NO_2), and HNO_3. HNO_3 makes up a small component of the total N, but is a sink of NO_x that is readily deposited to the surrounding ecosystem (Bytnerowicz and Fenn, 1996; Hanson and Lindberg, 1991). The timing of peak atmospheric reactive N concentration coincides with the dry season in southern California, due to dependence of HNO_3 production on photochemical reactions (Calvert et al., 1985), leading to a predominance of dry N deposition (Fenn et al., 2003). Once deposited, the N can alter ecosystem N cycling (Goulding et al., 1998) and affect competitive interactions among plants leading to vegetation type conversion (Allen et al., 2009; Padgett and Allen, 1999).

Once NO_x molecules are released to the atmosphere they undergo a series of photolytic reactions with ozone (O_3), peroxy radicals (R–O_2), and hydroxyl radicals to produce HNO_3 (Calvert et al., 1985). Industrial combustion releases NO_x with a positive $\delta^{15}N$ value (+3.8 to +20‰; Elliott et al., 2009; Felix et al., 2012), while vehicle emissions have been measured as both negative (−13‰ to −2‰; Heaton, 1990) or positive (+3.8‰ to +9‰; Ammann et al., 1999; Moore, 1977). The contradictory values have led to speculation that there may be secondary fractionation during the photolytic reactions leading to HNO_3 formation (Vicars et al., 2013). Atmospheric HNO_3 originating from natural processes, such as biogenic NO_x emissions (−27‰; Felix and Elliott, 2013) and lightning (0‰; Hoering, 1957), generally have lower $\delta^{15}N$ values relative to anthropogenic sources. While the HNO_3 $\delta^{15}N$ can be attributed to the source, the HNO_3 $\delta^{18}O$ is linked to the oxidation pathway leading to the production of HNO_3 (Hastings et al., 2003, 2004; Vicars et al., 2013). HNO_3 formed through 'nighttime' reactions with O_3 ($\delta^{18}O$ = 90–100‰) are more enriched in ^{18}O than HNO_3 molecules formed during 'daytime' reactions dominated by NO_2 reacting with OH radicals (Elliott et al., 2009; Jarvis et al., 2008).

Recent work by Vicars et al. (2013) has identified strong diurnal patterns in $\delta^{15}N$ values of atmospheric NO_x in the Los Angeles Basin. While some of this variation is due to changes in the relative contributions of HNO_3 sources, kinetic and equilibrium reactions (including gas–aerosol phase equilibria) involving NO_x, O_3, HNO_3, NH_3 and water vapor can potentially fractionate isotopes (Freyer, 1991; Freyer et al., 1993). The thermodynamics of these reactions is well established (Seinfeld and Pandis, 2006), but much less is known about their impact on the isotopic composition of HNO_3 in the atmosphere and how this will impact passive collection efforts. Measurements of temporal and spatial variation of the isotopic signature of HNO_3 can improve the understanding of varying sources and oxidation pathways of NO_x.

A national scale N deposition monitoring network run by the National Atmospheric Deposition Program (NADP) measures wet deposition across the continental US (NADP, 2012), while dry deposition of N in monitored by the US EPA's CASTNET monitoring network. (CASTNet, 2013). Dry deposition monitoring sites are concentrated in the eastern US, with relatively coarse coverage in the West (CASTNet, 2013). These gaps are filled for local analysis by simple, inexpensive passive sampling systems containing Nylasorb nylon filters (Bytnerowicz et al., 2005). These samplers allow monitoring of atmospheric HNO_3 concentration in specific areas of interest and can be used to calculate dry deposition rates through inferential methods (Clarke et al., 1997; Hanson and Lindberg, 1991). Isotopic analysis of collected HNO_3 may expand our understanding of N sources in the western US, but few studies have addressed the accuracy of the technique. Elliott et al. (2009) observed an offset (+6.4‰) in HNO_3 $\delta^{18}O$ values between actively and passively collected samples, suggesting that the passive samplers may be collecting biased isotopic measurements. This offset may have been associated with kinetic fractionation when HNO_3 adsorbs to the filters, fractionation of HNO_3 during extraction, or the co-collection of nitrous acid (HONO) on the filters (Bytnerowicz et al., 2005), but more study is needed.

The first objective of our study was to evaluate if passive samplers collect unbiased isotopologues of atmospheric HNO_3 under experimentally controlled HNO_3 concentrations. We hypothesized that the previously noted bias in isotopic measurements of passively collected HNO_3 will not occur under controlled laboratory conditions where the source isotopic signature can be held constant. The second question was whether sources of HNO_3 remained constant through space and time along a transect from the eastern portion of the highly polluted Los Angeles Air Basin eastward into the Sonoran Desert. We hypothesized that anthropogenic sources of NO_x would decline eastward toward the low deposition sites. Anthropogenic sources of NO_x are expected to be relatively weak at the low deposition sites, so we hypothesized that natural sources of NO_x, including lightning and soil emissions, would contribute a higher proportion of atmospheric HNO_3.

2. Methods

2.1. Continuously stirred tank reactors

Nylasorb filters (Pall Corporation, Port Washington, NY) were exposed to atmospheric HNO_3 with known concentrations and isotopic composition in continuously stirred tank reactors (CSTRs) to determine if isotopic fractionation of atmospheric HNO_3 occurs upon adsorption. Ambient air was pumped through an activated charcoal canister and a HEPA filter capsule (model 12144, Gelman Sciences, Ann Arbor, MI, U.S.A.) to remove background atmospheric contaminants before a concentrated HNO_3 solution (of $\delta^{15}N = 0.6 \pm 0.2$‰ and $\delta^{18}O = 26.0 \pm 0.2$‰) was volatilized and mixed with the airstream and pumped into the sealed chambers. For details of construction and operation of CSTRs, please refer to Padgett et al. (2004). The flow of the HNO_3 enhanced air simulated ambient conditions by creating daily peaks in HNO_3 values (high: 100 μg/m^3; moderate: 50 μg/m^3) in the mid-afternoon and then dropping back down near zero in the evening. The average 24 h concentrations in each chamber were 16 μg/m^3 and 8 μg/m^3 respectively, which bracketed measured field concentrations (4–12 μg/m^3). The concentration of the moderate chamber was determined based on the minimum flow rate at which the system produced consistent daily HNO_3 peaks while also maintaining consistent HNO_3 peaks in the high chamber.

HNO_3 within the chambers was measured with passive samplers of the Bytnerowicz et al. (2005) design. Ambient air diffuses through a 47 mm Zefluor PTFE Membrane filter of 2 μm pore-size (Pall Corporation) to a 47 mm Nylasorb nylon filter (HNO_3 collecting medium). All filters were loaded into passive samplers made of a 50 mm diameter Petri dish and capped with Petri dish lids to prevent any contamination prior to their deployment. Upon collection from the chambers, the filters were capped and stored at −20 °C.

Passive samplers were first deployed in September 2011 in four sets of three replicates. After the first week, one set of filters was collected while three additional sets continued to be exposed and three additional sets of filters were deployed. This pattern continued until four 1-week, three 2-week, two 3-week, and one 4-

week deployments were collected. Two filters were combined for each sample in the 1- and 2-week deployments for both chambers.

2.2. Field survey

2.2.1. Study site

The field sites were located in Riverside County, California, United States starting at the city of Riverside on the eastern edge of the Los Angeles Basin and moving east into the Sonoran Desert. Nitrogen deposition decreases in an eastward gradient from Riverside as N deposits and the contaminated air plume mixes with cleaner desert air (Allen et al., 2009; Fenn et al., 2010; Tonnesen et al., 2003). Nitric acid passive samplers were installed on September 1, 2011 along the N deposition gradient at 5 sites. Filters were exchanged every 7 days with the final filters being collected on September 29, 2011. One site was designated the 'source' site (Botanic Gardens, 13.1 kg/ha/yr) because it lies at the eastern edge of the Los Angeles air basin, two sites were in high deposition areas east of the Banning pass (Snow Creek, 15.6 kg/ha/yr; Whitewater; 17.6 kg/ha/yr), and two were in low deposition areas in Joshua Tree National Park, approximately 100 km to the east (Pinto Basin, 2.4 kg/ha/yr; Sunrise, 2.3 kg/ha/yr) (Fig. 1) (Tonnesen et al., 2003). Passive samplers were installed 2.4 m above the ground under PVC caps protecting the filters from contamination by rain and dust blowing at ground level.

2.2.2. Lightning

During the study, significant monsoonal rains occurred on September 5, 2011 (Week 1) and September 14, 2011 (Week 2) at all sites. Intense rainfall caused road damage preventing access to the two low N deposition sites for the third week of sampling. Counts of lightning strikes occurring during these events were obtained from the United States Precision Lightning Network which is administered by WSI Corporation and TOA Systems, Inc.

Rainfall appeared to contaminate some of the filters that were exposed during the second precipitation event as evidence by unusually high HNO_3 concentrations. These filters were measured for isotopic signature and all fell within a small range of both $\delta^{15}N$ and $\delta^{18}O$ values. The high sites had a $\delta^{18}O$ and $\delta^{15}N$ of 28.5 ± 1.1‰ and 1.7 ± 0.49‰ respectively, while the low sites had 20.1 ± 0.7‰ and 1.9 ± 0.1‰. Thus, the rainfall contaminated filters were removed from all data analyses.

2.3. Nitric acid analysis

Once all of the filters were collected, they were unloaded and placed in 125 ml polycarbonate Erlenmeyer flasks, to which 20 ml of deionized water was added prior to being shaken on a wrist-action shaker. The resulting filter extracts were decanted into a 20 ml HDPE scintillation vials and stored at −20 °C. The extracted solutions were analyzed for NO_3^- concentrations on a continuous flow analyzer (SEAL Analytical, Mequon, Wisconsin) using EPA Method 353.2. The total HNO_3 concentration (μg/m^3) was calculated using the NO_3^- concentration, the filter adsorption rate, and the length of time the filter was exposed to the atmosphere (Bytnerowicz et al., 2005). We considered the potential for isotopic fractionation of HNO_3 from the filters during the extraction process and discuss this.

The $\delta^{15}N$ and $\delta^{18}O$ of NO_3^- were measured using a bacterial method to convert NO_3^- into nitrous oxide (N_2O) at the Facility for Isotope Ratio Mass Spectrometer at UCR (Casciotti et al., 2002; Coplen et al., 2012). The bacteria Approximately 50 nmol of NO_3^- were added to bacterial cultures of *Pseudomonas aureofaciens* (ATCC# 13985) in sparged, sealed headspace vials. *P. aureofaciens* lacks N_2O reductase activity and therefore produces N_2O gas as a final product of denitrification which allows the $\delta^{15}N$ and $\delta^{18}O$ of NO_3^- to be determined simultaneously. The vials were inverted overnight to allow for complete conversion of NO_3^- while minimizing N_2O loss. The following morning, 0.1 ml of 10 N NaOH was added to each vial, before samples were directed into a gas chromatography column through a Thermo GasBench II (Thermo Fisher Scientific Inc., Waltham, MA) to separate the N_2O gas from residual CO_2. $\delta^{15}N$ and $\delta^{18}O$ values were measured using a Thermo Delta V isotope ratio mass spectrometer (Thermo Fisher Scientific Inc.). Reference standards, USGS-32, USGS-34 and USGS-35, were included in each analytical run to correct for instrument drift. Isotopic values are reported in per mill (‰) and were computed using Eqn. (1), where X = N or O. Isotopic values for oxygen are reported relative to VSMOW and nitrogen are reported relative to atmospheric N_2.

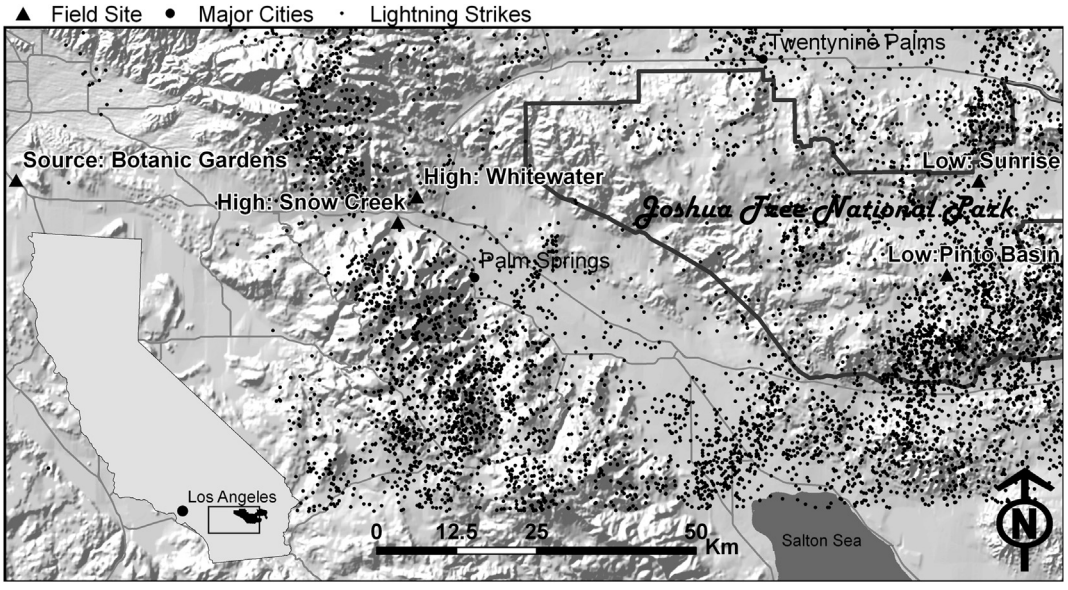

Fig. 1. Site locations of the 5 field sampling sites with lightning strikes occurring during sampling period.

$$X = \left(\frac{R_{Sample}}{R_{Standard}}\right) - 1 \quad (1)$$

2.4. Statistical analysis

The rate of HNO_3 collection in each chamber was determined by regressing the average dose of HNO_3 to the amount of HNO_3 collected by the filters. The slopes of the high and moderate chambers were compared by ANCOVA using HNO_3 dose as a covariate to determine if the concentration of atmospheric HNO_3 affected the rate of adsorption to the filters. A two-way ANOVA was used to test for the effects of site and deployment length on the amount of HNO_3 collected, and the $\delta^{15}N$ and $\delta^{18}O$ values of the extracted NO_3^-.

For the field samples, ANOVA was used to compare the effect of site location and timing of filter deployment and collection on atmospheric variables. A correlation analysis was conducted to measure the covariance between $\delta^{18}O$ and $\delta^{15}N$ on a single filter as well as the correlation between HNO_3 concentration and its isotopes. HNO_3 concentration data were inverse-transformed to achieve normality for among site analyses. An analysis of covariance effects test was then run for each site to evaluate difference in the correlation based on location. Data were analyzed using JMP software (Version 9.0 SAS Institute Inc.).

3. Results

3.1. Continuously stirred tank reactors

The amount of HNO_3 collected on the Nylasorb filters increased linearly with increasing HNO_3 dose in each chamber, with more variability at moderate doses (Fig. 2). The HNO_3 adsorption rate (ANCOVA df = 1, $F = 0.94$, $p = 0.33$) and amount of HNO_3 measured by combining two filters into a single sample (Moderate: df = 23, $F = 0.69$, $p = 0.41$; High: df = 23, $F = 2.90$, $p = 0.10$) were consistent in both chambers, allowing all samples to be pooled in the statistical analysis. Mean $\delta^{18}O$ and $\delta^{15}N$ values of HNO_3 collected from the filters of the high chamber ($\delta^{18}O = 25.8 \pm 0.3‰$ and $\delta^{15}N = 0.32 \pm 0.1‰$) were similar to those in the moderate chamber ($\delta^{18}O = 25.1 \pm 0.9‰$ and $\delta^{15}N = 0.4 \pm 0.1‰$) ($\delta^{18}O$, df = 1 $F = 0.55$ $p = 0.47$; $\delta^{15}N$, df = 1 $F = 1.24$ $p = 0.27$).

Results of ANOVA of CSTR data are presented in Table 1 and the mean values of the relationships in Fig. 3. In the moderate chamber the measured $\delta^{18}O$ value of HNO_3 started lower than expected in before increasing to values higher than the source solution as the deployment length increased. The $\delta^{18}O$ value in the high chamber remained consistent with expected values throughout deployments (Fig. 3A). The $\delta^{15}N$ values in both the high and the moderate chambers were lower than the source solution after one week deployments, but after three weeks, the mean $\delta^{15}N$ from both chambers was within 0.2‰ of the source solution (Fig. 3B). There was a two day malfunction in the CSTR chamber during the third week that led to HNO_3 not being volatilized. The filters that were deployed in the high chamber during this had a lower $\delta^{18}O$ value relative to previous deployments (Fig. 3C) and the $\delta^{15}N$ of these filters decreased, but not significantly (Fig. 4D).

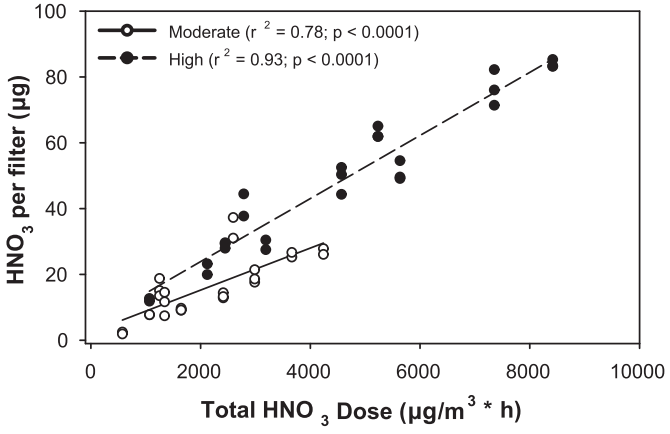

Fig. 2. Amount of HNO_3 collected per filter relative to the dose of HNO_3 to which they were exposed in two different concentrations of the continuously stirred tank reactors.

The bias of $\delta^{15}N$ and $\delta^{18}O$ relative to their expected values were not related on each filter. Temperature and humidity were not measured within the chambers, but a previous experiment, conducted at the same facility, observed chamber temperatures slightly higher than ambient conditions ($r^2 = 0.68$) and the humidity was slightly lower than ambient ($r^2 = 0.84$). Mean weekly ambient temperatures fluctuated between 21 and 24 °C during the experiment while mean weekly humidity fluctuated between 42 and 62%.

3.2. Field measurements

The results of the ANOVA of field data is presented in Table 1 and the means and significant differences among sites are presented in Table 2. HNO_3 concentration and $\delta^{18}O$ values were higher at the source and high deposition sites relative to the low deposition sites. The $\delta^{15}N$ value of HNO_3 was highest at the source site, then decreased at Snow Creek, and was lowest at the three eastern most sites. The number of lightning strikes within 10 km of the samplers was higher at the low sites (PB: 412 strikes, SM: 259 strikes) than the high (SC: 161 strikes, WW: 104 strikes) and the source site (BG: 1 strike) (Fig. 1). There was a decrease in the temperature and increase in humidity during week 2 and 3, with values returning to pre-storm conditions during Week 4 deployments (WRCC, 2013).

The results of ANOVAs for the effect of deployment week and week collected are presented in Table 1. The two high sites and two low sites were each combined for these analyses. Differences in values based on deployment week are presented in Table 3. There was an effect of deployment week on the $\delta^{18}O$ value, $\delta^{15}N$ value, and HNO_3 concentration at the source site and the high deposition sites, and on the $\delta^{18}O$ and $\delta^{15}N$ values at the low deposition sites. The HNO_3 concentration was higher during weeks 3 and 4 at the high deposition and source sites, while there was no difference in the amount collected at the low sites. The week 1 samples had higher $\delta^{18}O$ at the high and source sites, while week 1 and week 2 filters had similar $\delta^{18}O$ at the low sites. Week 4 filters had the lowest $\delta^{18}O$ at the high and low sites, while $\delta^{18}O$ for week 3 filters were lowest at the source site. $\delta^{15}N$ was highest during week 3 deployments at the high and source sites and week 4 samples at low sites. There was no relationship between the week collected and the $\delta^{18}O$, $\delta^{15}N$ at the sites. HNO_3 concentration was only different at the high and source sites during the first collection period before precipitation events had occurred.

Fig. 4 plots the $\delta^{15}N$ and $\delta^{18}O$ values of filters based on week collected (A) and deployment week (B) in dual isotope-ratio space. Outside of samples collected during the first week, samples from each site cluster based on site location based on the week collected. The site/week-deployed combinations form discrete groups within and among sites based on the deployment week.

Biplots of $\delta^{15}N$, $\delta^{18}O$ and HNO_3 concentration can be used to infer atmospheric processes along the depositional gradient. Keeling plots (plots of isotopic composition vs. $1/HNO_3$

Table 1
Results of Analysis of Variance of $\delta^{18}O$, $\delta^{15}N$, and HNO_3 dose for passive samplers in both CSTR and field experiments (df = degrees of freedom). The CSTR filters were analyzed independently for effects based on deployment week in the chamber as well as deployment length. The field sites were analyzed for the effect of site location, and then filters from each deposition region (Source, High, Low) were combined and analyzed by deployment week and week collected. Significant effects of ANOVA on $\delta^{18}O$, $\delta^{15}N$, and HNO_3 at $p < 0.05$ are in bold.

	Conc	$\delta^{18}O$			$\delta^{15}N$			HNO_3 concentration		
		df	F_{Value}	p	df	F_{Value}	p	df	F_{Value}	p
CSTR										
Deployment week	Mod	3	2.02	.0.14	3	0.53	0.66	3	2.76	0.07
	High	3	10.43	**<0.001**	3	0.94	0.44	3	5.51	**<0.01**
Deployment length	Mod	3	4.77	**<0.1**	3	3.15	**<0.05**	3	2.02	0.14
	High	3	0.96	0.43	3	3.18	**<0.05**	3	0.82	0.50
Field Study										
Site location	–	4	10.63	**<0.0001**	4	12.90	**<0.0001**	4	17.98	**<0.0001**
Deployment week	Source	3	4.15	**<0.05**	3	5.06	**<0.01**	3	4.76	**<0.01**
	High	3	12.50	**<0.0001**	3	4.14	**<0.05**	3	10.35	**<0.0001**
	Low	2	7.52	**<0.01**	2	3.92	**<0.05**	2	0.60	0.55
Week collected	Source	3	1.08	0.3740	3	2.05	0.1308	3	3.96	0.0184
	High	3	1.14	0.3416	3	0.50	0.6833	3	2.28	0.0908
	Low	2	0.07	0.9361	2	0.15	0.8573	2	0.08	0.9188

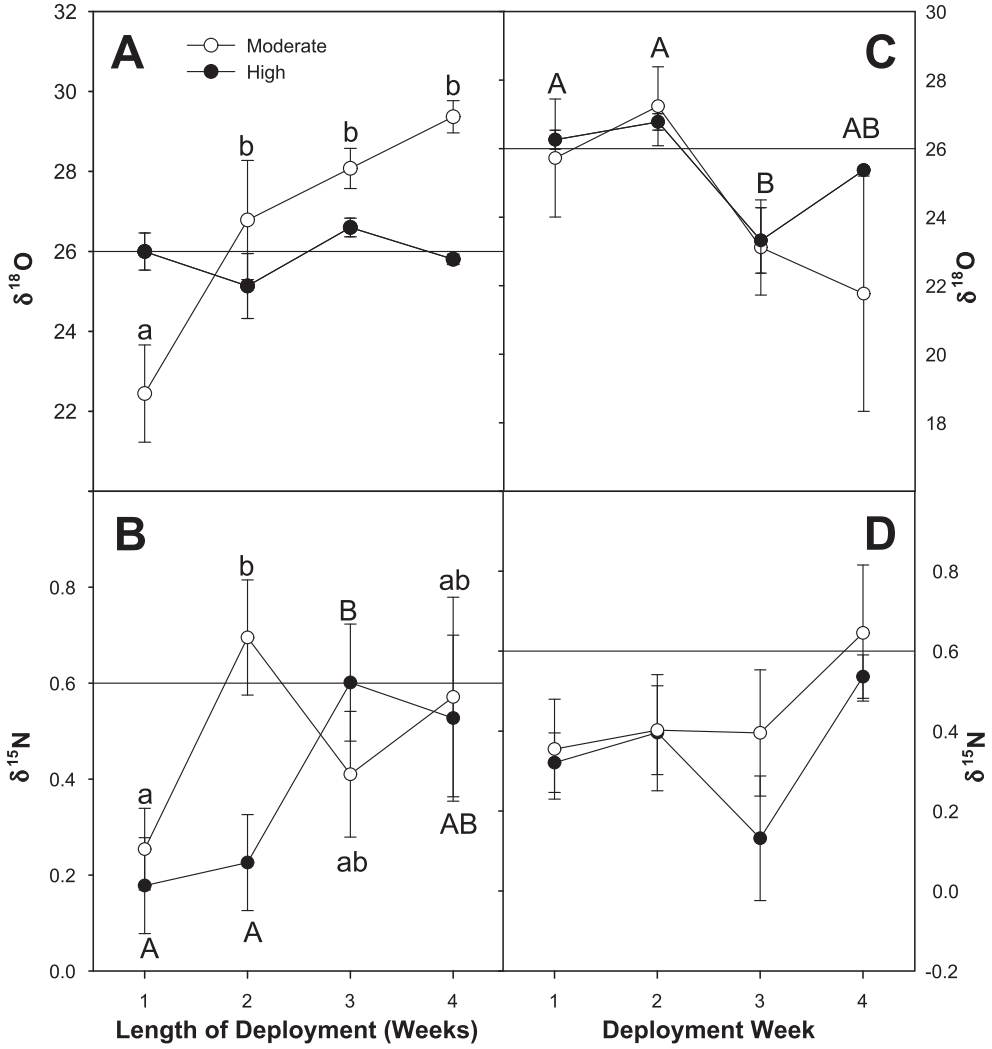

Fig. 3. Means of $\delta^{18}O$ (A) and $\delta^{15}N$ (B) of HNO_3 extracted from filters in the high and moderate CSTR chambers based on the deployment length and means of $\delta^{18}O$ (C) and $\delta^{15}N$ (D) of HNO_3 based on the deployment week. Horizontal lines represent $\delta^{18}O$ and $\delta^{15}N$ values of the stock HNO_3 solution that was volatilized and pumped into the chamber. Error bars represent the standard error of the mean. Capital letters represent differences in means in high chambers and lower case letters are differences in moderate chambers (Student's *t* test).

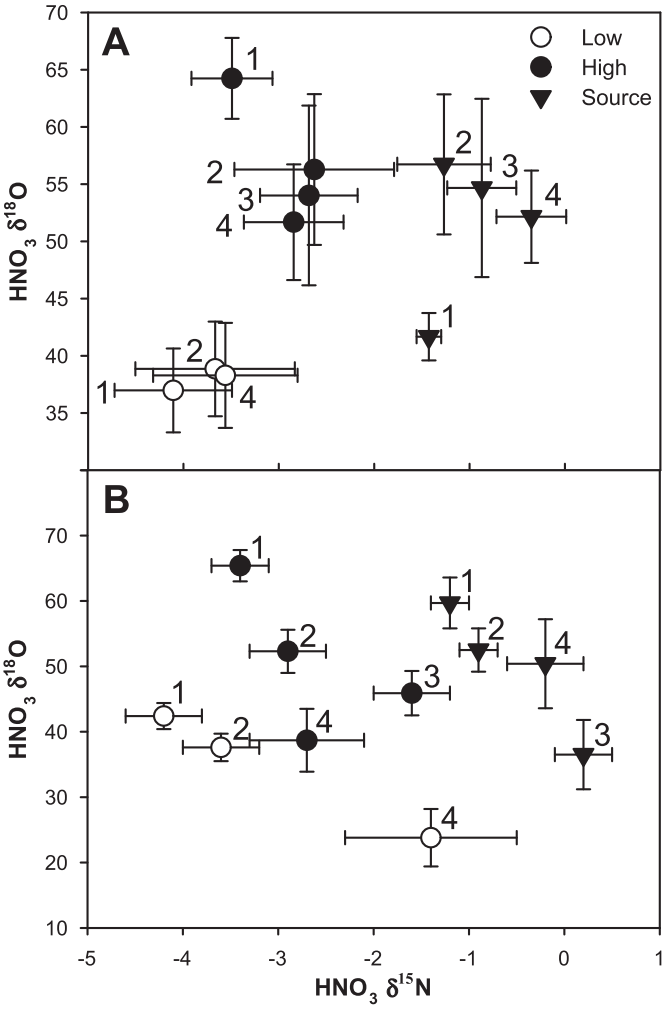

Fig. 4. Mean $\delta^{15}N$ and $\delta^{18}O$ values for filters based on the week that filters were collected (A) and the deployment week (B). Numbers signify the week of the filters were collected/deployed and error bars represent standard error of the mean.

concentration) are useful in identifying systems dominated by two-component mixing processes (Pataki et al., 2003). Since there were no significant differences in the slopes of the individual regressions between $\delta^{15}N$ and $\delta^{18}O$ for the two low sites (ANCOVA: $F = 1.36$, $p = 0.25$) or for the two high sites (ANCOVA: $F = 0.36$, $p = 0.55$), we present a single regression for the low sites and a single regression for the high sites in Fig. 5. The relationship between $\delta^{15}N$ and $\delta^{18}O$ was linear for each site (Fig. 5) and all of the slopes were statistically different (ANCOVA Effects test: $d = 3$, $F = 15.12$, $p < 0.0001$). The relationships between $\delta^{15}N$ and $\delta^{18}O$ relative to $1/HNO_3$ concentration were linear and varied independently among sites (Fig. 6).

Two-source mixing models were constructed independently for the high sites and the low sites for both $\delta^{15}N$ and $\delta^{18}O$ (Fig. 6). The 'shared endmember' for the two sites was estimated by extrapolating the two regression equations from high and low sites to their intercept for each element ($\delta^{18}O$ = 21.6‰ and $\delta^{15}N = -0.6$‰). The second endmember for each model was set as the largest $\delta^{18}O$ value and the lowest $\delta^{15}N$ value recorded at each site. The mean $\delta^{15}N$ and $\delta^{18}O$ of the 4-week deployment filters from the high and low sites were used to calculate a percent 'shared endmember' value. The two high sites had a mean percent 'shared endmember' of 41.6 ± 3.7% based on the $\delta^{18}O$ model and 39.3 ± 4.0% based on the $\delta^{15}N$ model. The low site had a 'shared endmember' value of 63.5 ± 4.1% based on the $\delta^{18}O$ model and 58.6 ± 4.4% based on the $\delta^{15}N$ model. Analysis of variance indicated a significant difference between high and low sites in the amount of 'shared endmember' N present based on both $\delta^{18}O$ (df = 1, $F = 17.66$, $p < 0.0001$) and $\delta^{15}N$ (df = 1, $F = 10.49$, $p < 0.005$) models. The source site was left out of this analysis due to the second endmember not trending toward the shared endmember isotopic signature.

4. Discussion

4.1. Utility of passive samplers for isotopic measurements of HNO_3

The Nylasorb filters in the high and moderate HNO_3 concentration chambers collected HNO_3 at a constant rate over a 4 week period without becoming saturated. This observation is consistent with previous studies conducted both outdoors and in CSTRs (Bytnerowicz et al., 2005). The isotopic signature of HNO_3 collected on Nylasorb filters relative to that of the source solution suggests that the atmospheric concentration of HNO_3 and the deployment length both impacted the isotopologues collected by the filters, although the mean $\delta^{18}O$ and $\delta^{15}N$ in each chamber were within 0.3‰ of the source HNO_3. The range of values measured was more confined for HNO_3 $\delta^{15}N$ (0‰–0.7‰) than HNO_3 $\delta^{18}O$ (22.4‰–27.0‰) which may have been due to changes in atmospheric chemistry within the chambers resulting from differences in temperature and UV radiation among deployments. The lack of relationship between the bias of $\delta^{15}N$ and $\delta^{18}O$ on individual filters indicates that there were no significant leaks in the system as this would have created a mixing of isotopologues toward a second source in both chambers.

The increased isotopic variation during shorter deployments in the moderate HNO_3 concentration chamber suggests that it may take longer than a week for an isotopic equilibrium to form between atmospheric HNO_3 and HNO_3 collected on the filters. There was a positive relationship between isotopologues of HNO_3 collected on synchronous 1-week filters in the high and moderate chambers suggesting that similar changes in background conditions were impacting both sets of filters, but had a larger impact in the moderate concentration chamber. The variability may have been caused by the atomic variability of HNO_3 coming in contact with the samplers at low concentrations as well as possible fractionation during the extraction process. There was no relationship between weekly variation in temperature and humidity, but daily fluctuations may have led to differences in adsorption rates. The source of HNO_3 was unchanged for the entire 4-week deployment,

Table 2
Differences in HNO_3 concentration and isotopic signature among sites. Values represent the mean of all filters exposed at a site and standard error of the mean. Significant differences among group means are indicated by superscript values (Student's *t*-test; $\alpha < 0.05$).

	Botanic	Snow creek	Whitewater	Pinto basin	Sunrise
HNO_3 concentration (μg/m^3)	10.4 ± 1.1^{1}	12.4 ± 1.2^{1}	10.5 ± 1.1^{1}	4.1 ± 1.2^{2}	5.3 ± 1.2^{2}
$\delta^{15}N$ (‰)	-0.8 ± 0.3^{A}	-2.2 ± 0.3^{B}	-3.3 ± 0.3^{C}	-4.0 ± 0.3^{C}	-3.5 ± 0.3^{C}
$\delta^{18}O$ (‰)	51.8 ± 2.4^{Y}	54.9 ± 2.6^{Y}	54.9 ± 2.6^{Y}	39.9 ± 3.1^{Z}	37.5 ± 2.8^{Z}

Table 3
Changes in HNO_3 concentration and HNO_3 isotopic signature along the N deposition gradient based on the deployment week. Analyses are among weeks and within sites. ANOVA was performed on inverse ($1/HNO_3$ concentration) values to normalize the data. Significant differences among group means are indicated by superscript values (Student's *t*-test; $\alpha < 0.05$).

		Week 1	Week 2	Week 3	Week 4
Source	HNO_3 concentration ($\mu g/m^3$)	10.2 ± 1.2^{1}	7.0 ± 1.1^{1}	17.0 ± 3.4^{2}	10.0 ± 1.6^{12}
	$\delta^{15}N$ (‰)	-0.9 ± 0.2^{AB}	-1.2 ± 0.2^{B}	0.2 ± 0.3^{C}	-0.2 ± 0.4^{AC}
	$\delta^{18}O$ (‰)	52.5 ± 3.3^{YZ}	59.7 ± 3.9^{Y}	36.5 ± 5.3^{Z}	50.4 ± 6.8
High	HNO_3 concentration	8.0 ± 0.4^{1}	9.5 ± 1.0^{1}	19.7 ± 3.4^{2}	11.8 ± 2.1^{1}
	$\delta^{15}N$	-3.4 ± 0.3^{A}	-2.9 ± 0.4^{A}	-1.6 ± 0.4^{B}	-2.7 ± 0.6^{AB}
	$\delta^{18}O$	65.4 ± 2.4^{X}	52.3 ± 3.3^{Y}	45.9 ± 3.4^{YZ}	38.7 ± 4.8^{Z}
Low	HNO_3 concentration	4.8 ± 0.6^{1}	4.3 ± 0.5^{1}		6.4 ± 2.4^{1}
	$\delta^{15}N$	-4.2 ± 0.4^{A}	-3.6 ± 0.4^{A}		-1.4 ± 0.9^{B}
	$\delta^{18}O$	42.4 ± 2.0^{Y}	37.6 ± 2.1^{Y}		23.8 ± 4.4^{Z}

limiting our ability to determine if there is any post adsorption exchange with atmospheric HNO_3.

The results of the CSTR portion of the experiment demonstrated that the Nylasorb filters effectively capture unbiased isotopologues of atmospheric HNO_3 in controlled atmospheric conditions if given sufficient time to equilibrate. Filters deployed in the moderate chambers for one week had a lower $\delta^{18}O$ value than the source solution, so a two week exposure is recommended to obtain an accurate measurement. While rates of dry deposition of atmospheric HNO_3 to soil and plant surfaces are affected by changes in temperature and humidity (Brook et al., 1999), variations in temperature and humidity in the CSTRs did not have an effect on changes in isotopologue accumulation on the filter. This finding suggests that changes in accumulation that occurred in the field were the result of changes in atmospheric concentrations associated with changing sources of HNO_3.

4.2. Field measurements

The HNO_3 concentrations recorded at the high field sites were similar to previously measured levels, while the low sites increased from 2.5 to 3.5 $\mu g/m^3$ (Allen et al., 2009; Rao et al., 2009). The increase may have been related to the precipitation events which did not occur during previous deployments. The baseline isotopic signature of atmospheric HNO_3 (Week 1 deployment, 1-week exposure) was unique at the source, high, and low sites. The $\delta^{15}N$ values of all samples were negative (−1.1‰ to −5.6‰) suggesting that the main source of anthropogenic HNO_3 was automotive (Heaton, 1990). This is consistent with emissions data from Los Angeles where over 50% of NO_x comes from automotive combustion (CARB, 2009). The largest $\delta^{18}O$ values recorded at each set of sites were consistent with previously measured atmospheric values (Elliott et al., 2009; Hastings et al., 2004). The $\delta^{15}N$ and $\delta^{18}O$ values both decreased from west to east. The depletion of heavy isotopologues from the LA Basin eastward could be caused by preferential loss of heavier isotopologues along the gradient. The high deposition sites are directly in the path of air moving out of the Los Angeles Air Basin, while the low deposition sites are protected from

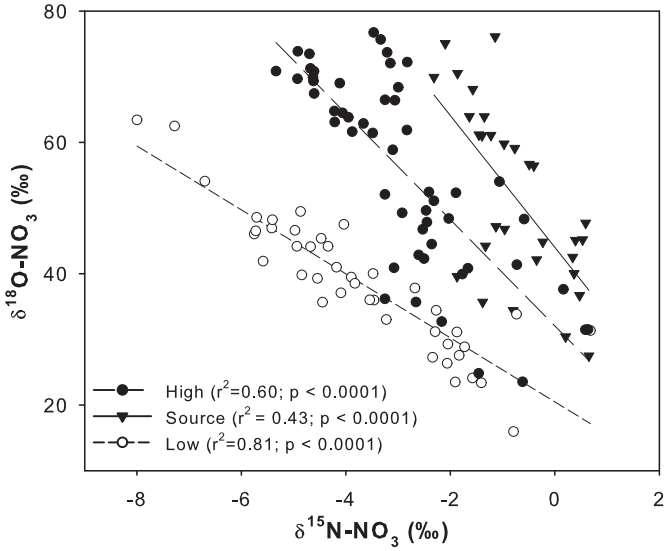

Fig. 5. The relationship between the $\delta^{18}O$ value and $\delta^{15}N$ value of passively collected HNO_3 on individual filters separated by deposition intensity.

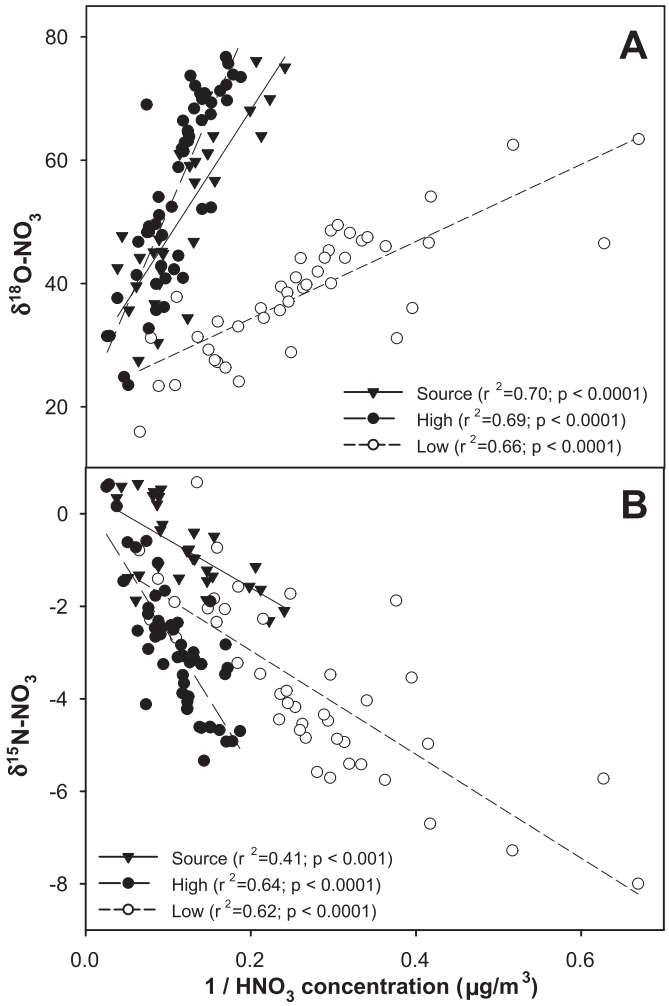

Fig. 6. The $\delta^{18}O$ (A) and $\delta^{15}N$ (B) values of passively collected HNO_3 are correlated with the amount of HNO_3 collected on each filter.

direct flow by the Little San Bernardino Mountains which limit mixing of air masses from the valley. As the anthropogenic HNO_3 molecules are deposited, a larger proportion of biogenic nitrate molecules lead to an overall depletion of ^{15}N isotopologues in the atmosphere.

Another possible cause of the difference in isotopologues at each end of the gradient is the fractionation of ^{15}N during the formation and loss of HNO_3 along the gradient. While the photochemistry of HNO_3 along the deposition gradient was beyond the scope of this study, we speculate that equilibrium reactions between gas and aerosol phases of HNO_3, including the formation of NH_4NO_3 aerosols, may partially explain this trend. Because we learned that Nylasorb filters collect unbiased isotopologues, further studies can be conducted during stable atmospheric conditions combining O_3, NO, and NO_2 measurements to help determine the fate of HNO_3.

The contribution of HONO is also unknown at each site. The HNO_3:HONO has been measured as low as 2.3:1 within the city of Riverside (Bytnerowicz et al., 2005), but is expected to be high in rural areas such as San Gabriel Mountains (40:1) and the San Bernardino Mountains (21:1) downwind of Los Angeles (Bytnerowicz and Fenn, 1996; Seinfeld and Pandis, 2006). We assume that the N in both HONO and HNO_3 collected on the filter originated from the same NO_x source, thus the $\delta^{15}N$ of HONO and HNO_3 would be at isotopic equilibrium. It is also likely that HONO and HNO_3 share at least one common O atom. Since HONO is formed through the reaction between NO_x and either H_2O ($\delta^{18}O < -5‰$; based on precipitation values) or OH ($\delta^{18}O$ equivalent to water vapor (Lyons, 2001)), we would expect HONO to have a lower $\delta^{18}O$ relative to HNO_3 due to the greater role of O_3 molecules in HNO_3 production ($\delta^{18}O \approx +90‰$; Jarvis et al., 2008). If HONO was slightly higher in the low deposition sites, increased OH radicals in HONO could have contributed to lower $\delta^{18}O$ values.

The deployments immediately following the rain event collected more HNO_3 at the high and source sites than those deployed during the first two weeks. Previous CSTR chamber experiments have shown an increase in HNO_3 adsorption under high humidity, but not of the same magnitude measured in this experiment (Padgett, 2010), suggesting that the change in concentration was due to an increase in ambient HNO_3. The two main factors that could increase the amount of ambient HNO_3 in the desert are soil NO_x emissions and lightning. The wetting of dry desert soil leads to pulses of biogenic NO_x (McCalley and Sparks, 2009), however; soil emissions of NO_x are expected to have depleted $\delta^{15}N$ values due to preferential fractionation of lighter isotopes (Felix and Elliott, 2013), while the $\delta^{18}O$ value would be consistent with other atmospheric values due to the same oxidation pathway. Summer monsoons in the region tend to have a significant amount of lightning, which can produce 3.5 kg N per flash (Schumann and Huntrieser, 2007) dominated by NO_x (Hastings et al., 2003; Tie et al., 2001). NO_x is produced in the lightning channel by the Zel'dovich mechanism from the breakup of N_2 and O_2 molecules (Zel'dovich and Raizer, 1966). The $\delta^{18}O$ of atmospheric O_2 is 23.5‰ (Kroopnick and Craig, 1972) and the $\delta^{15}N$ of atmospheric N_2 is 0‰. This pulse of NO_x can be rapidly converted to HNO_3 in the lower troposphere (Tie et al., 2001), which leads us to conclude that HNO_3 from lightning is mixing directly at each site with the background HNO_3 from anthropogenic sources. The lightning HNO_3 had a larger impact on atmospheric concentrations at the low deposition sites relative to the high deposition sites due to the lower background HNO_3 concentrations present before and after the storms moved through (Fig. 5). A two source mixing model determined that lightning created $63.5 \pm 4.1\%$ of the HNO_3 at the low sites compared with $41.6 \pm 3.7\%$ at the high sites.

The only hesitation we have in attributing the second source to lightning is the continued mixing present in the filters deployed during the fourth week. During these deployments, the isotopologues of HNO_3 began to return to their pre-storm values at the source and high sites, while the low sites remained near the lightning value. The road to the low site was washed out by the rain events and subsequently closed, which reduced local traffic and therefore anthropogenic NO_x emissions. This suggests that there is a lingering effect of the precipitation event on atmospheric HNO_3 concentration. A pulse of HNO_3 from a lightning strike would not be expected to remain in the air column for any significant amount of time due to air mass movement and the mean residence time of HNO_3 in the atmosphere. An alternate hypothesis is that the precipitation event changed the rate of HONO formation and led to more HONO being collected on the filter than HNO_3. Further research is needed to measure HONO as well as the isotopic signature of soil emissions following the wetting of soil and whether or not they are affected by lightning strikes.

Due to the contribution of the lightning HNO_3, the filters were exposed to atmospheric conditions with a varying dominant source of HNO_3. The initial atmospheric conditions affected the final isotopic signature of the collected HNO_3. The strong separation of mean values based on date of first deployment along dual isotopic space suggests that the isotopologues collected during the initial deployment period have a disproportionate impact on the final isotopic signature of the sample (Fig. 4). Given that the highest concentrations of HNO_3 were collected on the week 3 samples at the high and source site (Table 3), it could be assumed that the filters exposed during this period would have the largest influence on the total HNO_3 $\delta^{15}N$ and $\delta^{18}O$. This is not a function of saturation of the filter, as the CSTR showed that under controlled conditions, there HNO_3 adsorption increased linearly through time (Fig. 2). Since there was no relationship between the date the filters were collected and the isotopic signature of those filters, it is assumed that the adsorption of HNO_3 to the filters is limited over time. This may have been due to dust particles collecting on the PTFE filter that controls air diffusion to the Nylasorb (Bytnerowicz et al., 2005). Future experiments should measure the amount of HNO_3 collected on the PTFE filter to determine if fractionation is occurring. In the same vein, the linear mixing of isotopes collected on the filters at each of the sites suggests that there is not significant exchange of isotopologues of HNO_3 bound to the filter with those in the atmosphere.

The $\delta^{15}N$ and $\delta^{18}O$ values collected during week 4 at the source site indicate that atmospheric HNO_3 was returning toward its normal composition more quickly than the desert sites. This may be the result of the source site sampler being located 1.5 km from a major freeway where it was exposed to a consistent input of NO_x. The source site also did not receive as much precipitation during the deployment period as the other sampling sites.

The variation measured in weekly field samples increases the need to experimentally alter the source HNO_3 solution in the CSTR. Alternating between spiked and standard HNO_3 solutions would mimic the pulses of HNO_3 added to the atmosphere by lightning strikes and verify our two source mixing models. It may also prove to be beneficial to alter humidity, wind speed, and wetness of the filter in the CSTR to determine if conditions present during and following a precipitation event bias adsorption of isotopologues.

5. Conclusions

The results of this experiment suggest that Nylasorb filters are an effective means of collecting atmospheric HNO_3 for isotopic analysis. Under stable conditions the filters can collect accurate, consistent measurements of HNO_3 $\delta^{18}O$ and $\delta^{15}N$. Based on field results, during longer exposures, the filters may bias toward isotopologues present at the initial deployment conditions due to dust collection on the samplers. A two-week field deployment appears

to be the most effective timing to gather accurate isotopic data. This deployment length in the CSTRs produced average isotopic ratios within 0.5‰ of the true value for both $\delta^{18}O$ and $\delta^{15}N$. Using a two-week deployment minimizes the amount of variability in the isotopic ratios data for both elements while increasing the ability to plan the deployment around variable weather patterns. This also limits the impact that dust accumulation could have air diffusion to the filter surface.

The storms with lightning events that occurred during the study period created variable isotopic ratios of HNO_3 during the multiple deployment periods. The mixing of isotopologues was indicative of a two-source mixing model with a shared second source among the high and low deposition sites. We attributed this shared source to HNO_3 created by lightning strikes based on the similarity of N and O isotopic signatures of N and O with their atmospheric constituents. Future CSTR chamber studies should use an HNO_3 isotope tracer to simulate a pulse of a second HNO_3 source into a stable atmosphere to verify how the filters adsorb isotopologues of two sources of HNO_3.

Acknowledgments

This research was made possible by grants from the National Science Foundation (DEB-1110832) and the San Bernardino Community Foundation Desert Research Fund. The authors would like to thank Josh Hoines and Katie Kain from Joshua Tree National Park and Katie O'Conner from the Friends of the Desert Mountains for assistance with site access and Delores Lucero, Diane Alexander, Elizabeth Hessom, Ben Wissinger, and Taahira Major for field and lab assistance. We would also like to thank the two anonymous reviewers for their comments on the initial submission.

References

Allen, E.B., Rao, L.E., Steers, R.J., Bytnerowitcz, A., Fenn, M.E., 2009. Impacts of atmospheric nitrogen deposition on vegetation and soils in Joshua Tree National Park. In: Webb, R.H., Fenstermaker, L.F., Heaton, J.S., Hughson, D.L., McDonald, E.V., Miller, D.M. (Eds.), The Mojave Desert: Ecosystem Processes and Sustainability. University of Nevada Press, Las Vegas, pp. 78–100.

Ammann, M., Siegwolf, R., Pichlmayer, F., Suter, M., Saurer, M., Brunold, C., 1999. Estimating the uptake of traffic-derived NO_2 from N-15 abundance in Norway spruce needles. Oecologia 118, 124–131.

Brook, J.R., Zhang, L., Li, Y., Johnson, D., 1999. Description and evaluation of a model of deposition velocities for routine estimates of dry deposition over North America. Part II: review of past measurements and model results. Atmos. Environ. 33, 5053–5070.

Bytnerowicz, A., Fenn, M.E., 1996. Nitrogen deposition in California forests: a review. Environ. Pollut. 92, 127–146.

Bytnerowicz, A., Sanz, M.J., Arbaugh, M.J., Padgett, P.E., Jones, D.P., Davila, A., 2005. Passive sampler for monitoring ambient nitric acid (HNO3) and nitrous acid (HNO_2) concentrations. Atmos. Environ. 39, 2655–2660.

Calvert, J.G., Lazrus, A., Kok, G.L., Heikes, B.G., Walega, J.G., Lind, J., Cantrell, C.A., 1985. Chemical mechanisms of acid generation in the troposphere. Nature 317, 27–35.

California Air Resources Board (CARB), 2009. Emission Data by Region (Statewide), California Air Resources Board. Retrieved from: http://www.arb.ca.gov/ei/emissiondata.htm.

Casciotti, K.L., Sigman, D.M., Hastings, M.G., Böhlke, J.K., Hilkert, A., 2002. Measurement of the oxygen isotopic composition of nitrate in Seawater and freshwater using the denitrifier method. Anal. Chem. 74, 4905–4912.

CASTNet (Clean Air Status and Trends Network), 2013. Annual Report, p. 2011. Retrieved from: http://epa.gov/castnet/javaweb/docs/annual_report_2011.pdf.

Clarke, J.F., Edgerton, E.S., Martin, B.E., 1997. Dry deposition calculations for the clean air status and trends network. Atmos. Environ. 31, 3667–3678.

Coplen, T.B., Qi, H., Révész, K., Casciotti, K., Hannon, J.E., 2012. Determination of the $\delta^{15}N$ and $\delta^{18}O$ of nitrate in water; RSIL lab code 2900. Chap. 17. In: Révész, Kinga, Coplen, T.B. (Eds.), Stable Isotope-Ratio Methods, Sec. C, Methods of the Reston Stable Isotope Laboratory: U.S. Geological Survey Techniques and Methods, Book 10, p. 35. Available only at: http://pubs.usgs.gov/tm/2006/tm10c17/.

Elliott, E.M., Kendall, C., Boyer, E.B., Burns, D.A., Lear, G., Golden, H.E., Harlin, K., Bytnerowicz, A., Butler, T.J., Glatz, R., 2009. Dual nitrate isotopes in dry deposition: utility for partitioning NO_x source contributions to landscape nitrogen deposition. J. Geophys. Res. Biogeosci. 114, G04020.

Felix, J.D., Elliott, E.M., 2013. The agricultural history of human-nitrogen interactions as recorded in ice core $\delta^{15}N$-NO_3^-. Geophys. Res. Lett. 40, 1642–1646.

Felix, J.D., Elliott, E.M., Shaw, S.L., 2012. Nitrogen isotopic composition of coal-fired power plant NO_x: influence of emission controls and implications for global emission inventories. Environ. Sci. Technol. 46, 3528–3535.

Fenn, M.E., Allen, E.B., Weiss, S.B., Jovan, S., Geiser, L.H., Tonnesen, G.S., Johnson, R.F., Rao, L.E., Gimeno, B.S., Yuan, F., Meixner, T., Bytnerowicz, A., 2010. Nitrogen critical loads and management alternatives for N-impacted ecosystems in California. J. Environ. Manag. 91, 2404–2423.

Fenn, M.E., Haeuber, R., Tonnesen, G.S., Baron, J.S., Grossman-Clarke, S., Hope, D., Jaffe, D.A., Copeland, S., Geiser, L., Rueth, H.M., Sickman, J.O., 2003. Nitrogen emissions, deposition, and monitoring in the western United States. Bioscience 53, 391–403.

Freyer, H.D., 1991. Seasonal-variation of N15/N14 ratios in atmospheric nitrate species. Tellus Ser. B Chem. Phys. Meteorol. 43, 30–44.

Freyer, H.D., Kley, D., Volzthomas, A., Kobel, K., 1993. On the interaction of isotopic exchange processes with photochemical-reactions in atmospheric oxides of nitrogen. J. Geophys. Res. Atmos. 98, 14791–14796.

Galloway, J.N., Aber, J.D., Erisman, J.W., Seitzinger, S.P., Howarth, R.W., Cowling, E.B., Cosby, B.J., 2003. The nitrogen cascade. Bioscience 53, 341–356.

Goulding, K.W.T., Bailey, N.J., Bradbury, N.J., Hargreaves, P., Howe, M., Murphy, D.V., Poulton, P.R., Willison, T.W., 1998. Nitrogen deposition and its contribution to nitrogen cycling and associated soil processes. New. Phytol. 139, 49–58.

Hanson, P.J., Lindberg, S.E., 1991. Dry deposition of reactive nitrogen compounds: a review of leaf, canopy and non-foliar measurements. Atmos. Environ. Part A General Top. 25, 1615–1634.

Hastings, M.G., Sigman, D.M., Lipschultz, F., 2003. Isotopic evidence for source changes of nitrate in rain at Bermuda. J. Geophys. Res. 108, 4790.

Hastings, M.G., Steig, E.J., Sigman, D.M., 2004. Seasonal variations in N and O isotopes of nitrate in snow at Summit, Greenland: implications for the study of nitrate in snow and ice cores. J. Geophys. Res. 109, D20306.

Heaton, T.H.E., 1990. 15N/14N ratios of NO_x from vehicle engines and coal-fired power stations. Tellus B 42, 304–307.

Hoering, T., 1957. The isotopic composition of the ammonia and the nitrate ion in rain. Geochim. Et. Cosmochim. Acta 12, 97–102.

Jarvis, J.C., Steig, E.J., Hastings, M.G., Kunasek, S.A., 2008. Influence of local photochemistry on isotopes of nitrate in Greenland snow. Geophys. Res. Lett. 35, L21804.

Kroopnick, P., Craig, H., 1972. Atmospheric oxygen: isotopic composition and solubility fractionation. Science 175, 54–55.

Lyons, J.R., 2001. Transfer of mass-independent fractionation in ozone to other oxygen-containing radicals in the atmosphere. Geophys. Res. Lett. 28, 3231–3234.

McCalley, C.K., Sparks, J.P., 2009. Abiotic gas formation drives nitrogen loss from a desert ecosystem. Science 326, 837–840.

Moore, H., 1977. Isotopic composition of ammonia, nitrogen-dioxide, and nitrate in atmosphere. Atmos. Environ. 11, 1239–1243.

NADP, 2012. National Atmospheric Deposition Program 2011 Annual Summary, NADP Data Report 2012-01. Illinois State Water Survey.

Padgett, P.E., 2010. The effect of ambient ozone and humidity on the performance of nylon and Teflon filters used in ambient air monitoring filter-pack systems. Atmos. Pollut. Res. 1, 23–29.

Padgett, P.E., Allen, E.B., 1999. Differential responses to nitrogen fertilization in native shrubs and exotic annuals common to Mediterranean coastal sage scrub of California. Plant Ecol. 144, 93–101.

Padgett, P.E., Bytnerowicz, A., Dawson, P.J., Riechers, G.H., Fitz, D.R., 2004. Design, evaluation and application of a continuously stirred tank reactor system for use in nitric acid air pollutant studies. Water Air Soil Pollut. 151, 35–51.

Pataki, D.E., Ehleringer, J.R., Flanagan, L.B., Yakir, D., Bowling, D.R., Still, C.J., Buchmann, N., Kaplan, J.O., Berry, J.A., 2003. The application and interpretation of keeling plots in terrestrial carbon cycle research. Glob. Biogeochem. Cycles 17.

Rao, L.E., Parker, D.R., Bytnerowicz, A., Allen, E.B., 2009. Nitrogen mineralization across an atmospheric nitrogen deposition gradient in Southern California deserts. J. Arid Environ. 73, 920–930.

Schumann, U., Huntrieser, H., 2007. The global lightning-induced nitrogen oxides source. Atmos. Chem. Phys. 7, 3823–3907.

Seinfeld, J.H., Pandis, S.N., 2006. Atmospheric Chemistry and Physics: from Air Pollution to Climate Change, second ed. John Wiley & Sons, Inc., New York.

Templer, P.H., Weathers, K.C., 2011. Use of mixed ion exchange resin and the denitrifier method to determine isotopic values of nitrate in atmospheric deposition and canopy throughfall. Atmos. Environ. 45, 2017–2020.

Tie, X., Zhang, R., Brasseur, G., Emmons, L., Lei, W., 2001. Effects of lightning on reactive nitrogen and nitrogen reservoir species in the troposphere. J. Geophys. Res. Atmos. 106, 3167–3178.

Tonnesen, G.S., Wang, Z.S., Omary, M., Chien, C.J., 2003. Model simulations of formation, transport and deposition of ozone, fine particulates and nitrates in the Sierra Nevada. In: Bytnerowicz, A., Arbaugh, M., Alonso, R. (Eds.), Ozone Air Pollution in the Sierra Nevada – Distribution and Effects on Forests. Developments in Environmental Sciences. Elsevier Press, Amsterdam, Netherlands.

Vicars, W.C., Morin, S., Savarino, J., Wagner, N.L., Erbland, J., Vince, E., Martins, J.M.F., Lerner, B.M., Quinn, P.K., Coffman, D.J., Williams, E.J., Brown, S.S., 2013. Spatial and diurnal variability in reactive nitrogen oxide chemistry as reflected in the

isotopic composition of atmospheric nitrate: results from the CalNex 2010 field study. J. Geophys. Res. Atmos. 118, 10,567–10,588.
Vitousek, P.M., Aber, J.D., Howarth, R.W., Likens, G.E., Matson, P.A., Schindler, D.W., Schlesinger, W.H., Tilman, D.G., 1997. Human alteration of the global nitrogen cycle: sources and consequences. Ecol. Appl. 7, 737–750.
WRCC (Western Regional Climate Center), 2013. Palm Springs, CA (046635), Monthly Climate Summary, 9/1/2011 to 9/28/2011. Website: http://www.wrcc.dri.edu.
Zel'dovich, Y.B., Raizer, Y.P., 1966. Physics of Shock Waves and High-temperature Hydrodynamic Phenomena. Academic Press, New York.